Theory of local-phonon-coupled low-energy anharmonic excitation of the interstitial oxygen in silicon

Hiroshi Yamada-Kaneta
Basic Process Development Division, Electronic Devices Group, Fujitsu Limited, 1015 Kamikodanaka, Nakahara-ku, Kawasaki 211, Japan

Chioko Kaneta
Semiconductor Devices Laboratory, Fujitsu Laboratories Limited, 10-1 Morinosato-Wakamiya, Atsugi 243-01, Japan

Tsutomu Ogawa
Basic Process Development Division, Electronic Devices Group, Fujitsu Limited, 1015 Kamikodanaka, Nakahara-ku, Kawasaki 211, Japan
(Received 12 February 1990; revised manuscript received 19 June 1990)

The previous model for the low-energy anharmonic excitation of the interstitial oxygen in silicon [D. R. Bosomworth, W. Hayes, A. R. L. Spray, and G. D. Watkins, Proc. R. Soc. London, Ser. A **317**, 133 (1970)] is expanded so that the coupling to the local phonon is included. The result of the calculation explains the previously observed absorption peaks of ^{16}O and ^{18}O in the 30-, 1100-, and 1200-cm^{-1} bands, confirming the energy-level scheme and transition assignment of Bosomworth *et al.* The coupling significantly reduces the level separations of the low-energy anharmonic excitation, and plays an important role in explaining the ^{18}O isotope peak shifts. A physical interpretation is given to the calculated negative coupling constant. The origin of the 517- and 1700-cm^{-1} bands is also discussed.

I. INTRODUCTION

The $\langle 111 \rangle$ bond-interstitial oxygen (O_i) in silicon[1-3] causes the series of infrared and far-infrared impurity absorption bands shown in Table I.[1-10] These bands, except the 517-cm^{-1} one, consist of a group of peaks (multipeak structure) that exhibit strong temperature dependence at about 10–50 K.[1,2,4-6,9]

Bosomworth *et al.*[5] showed that the O_i is an off-center impurity[11,12] whose (x,y) freedom of motion (Fig. 1) causes the two-dimensional (2D) low-energy anharmonic excitation (LEAE). They assigned the 30-cm^{-1} band to the transitions between the calculated LEAE multiplets belonging to the zero-ν_3-phonon state.[5] They further determined experimentally the levels of the LEAE multiplets belonging to the one-ν_3-phonon state (Fig. 9 of Ref. 5). The 1100- and 1200-cm^{-1} bands were assigned to the transitions between the zero- and one-ν_3-phonon states.[5] They ascribed the 1200-cm^{-1} band to the multiquantum transitions due to the coupling of the LEAE to the ν_3 local phonon.[5] They also attributed the multipeak structure of the 1100-cm^{-1} band to such an effect (of the coupling) that the energy-level separation of the LEAE in the one-phonon state becomes smaller than in the zero-phonon state.[5] We confirm these results and suggestions of Bosomworth *et al.*,[5] formulating the local-phonon coupling which consistently describes both of the zero- and one-phonon LEAE multiplets. Our model is an expansion of the model of Bosomworth *et al.*,[5] which treated only the 2D LEAE. The double-peak structures due to the $\langle 111 \rangle$-oriented acceptor-hydrogen complexes in silicon[13] may be due to the analogous effect of the coupling.

Bosomworth *et al.*[5] overestimated the ^{18}O isotope shifts of the 29.3- and 37.8-cm^{-1} peaks by the 2D one-body excitation model for the O_i in the static host lattice. They took into account only the mass difference between ^{16}O and ^{18}O, neglecting the coupling to other freedoms of lattice excitation.[5] We refer to such a model as the free 2D LEAE model. We try to resolve the overestimation taking the local-phonon coupling into account.

The absorption bands have often been assigned to or discussed with the normal vibrations in the bent Si ⁄ O ＼ Si virtual molecule with C_{2v} symmetry.[1,5,7-9] This is a misleading modeling. In the LEAE, an off-center Si ⁄ O ＼ Si configuration, which is stable in the statical point of view, quickly changes to the oppositely bent Si ＼ O ⁄ Si configuration by the radial motion of O, as well as by z-axial rotation. Therefore, these normal vibrations formally considered for one of the equivalent off-center configurations are not physically meaningful. To unambiguously describe the excitations, we adopt the D_{3d} configuration as the origin of the atomic displacements. We first separate all degrees of freedom of atomic motion into two systems: the 2D LEAE of the O_i, and a system of phonons including the high-energy impurity modes. We then take into account the relevant interaction terms between the two systems: the local-phonon couplings.

The paper includes a detailed description of our previ-

TABLE I. Previously observed low-temperature infrared and far-infrared absorptions due to the interstitial oxygen in silicon. The absorption peaks due to $^{28}Si—^{16}O—^{28}Si$ (second column) and $^{28}Si—^{18}O—^{28}Si$ (third column) are classified into the bands in the first column. The fourth column shows the initial state of the transition corresponding to each peak, which is determined from the observed temperature dependence of the peak intensity. The symbol G (E) indicates the ground state (an excited state); the E' excited state is lower in energy than the E'' excited state. The fifth column shows the symmetry of the irreducible transition dipole operator(s) associated with each band, which is determined from the measured stress-induced dichroism.

Absorption bands (cm^{-1})	Wave numbers of the observed peaks (cm^{-1}) ^{16}O	^{18}O	Initial state	Symmetry of transition dipole(s)
30[a]	29.3	27.2	G	
	37.8	35.3	E	(x,y)
	43.3		E	
	49.0		E	
517[b]	517.3	517.3	G	(x,y)[f]
1100[a,b,c]	1136.0	1084.4	G	
	1127.8	1076.7	E'	z[a,g]
	1122.0	1071.0	E''	
1200[a,b,d]	1203.0	1150.8	G	z[a]
	1216.8		E	
1700[e]	1748.6		G	
	1741.2		E'	z[h]
	1735.5		E''	

[a]Reference 5.
[b]Table I in Ref. 2.
[c]References 1 and 4.
[d]References 8 and 9.
[e]References 6, 8, and 9.
[f]Reference 7.
[g]Reference 3.
[h]Reference 10.

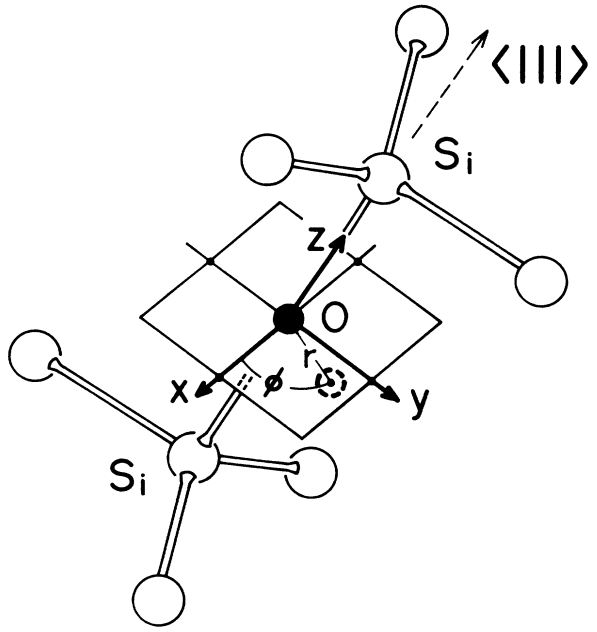

FIG. 1. The D_{3d} atomic configuration and the Cartesian coordinate axes. The origin of the coordinate axes is at the center of symmetry; the z axis is parallel to the ⟨111⟩ crystallographic axis. This coordinate system is used all through this paper. The displaced oxygen atom is also described by a dashed circle.

ous publication.[14] In Sec. II, we introduce the local-phonon-coupling model to describe the 30-, 1100- and 1200-cm^{-1} bands. The Schrödinger equation is reduced to that for the local-phonon-renormalized 2D LEAE, and solved numerically. In Sec. IV, we obtain, for both ^{16}O and ^{18}O, the energy levels consistent with experiment. We explain how the coupling gives rise to the 1200-cm^{-1} band and the multipeak structure of the 1100-cm^{-1} band. We calculate the relative intensities of the 1200-cm^{-1}-band peaks. The coupling is shown to be an important factor in explaining the isotope peak shifts. In Sec. V, we explain the physical origin of the calculated negative coupling constant. We discuss the origin of the 517- and 1700-cm^{-1} absorptions.

II. MODEL AND METHOD OF CALCULATION

We consider a silicon crystal containing a single O_i, and take, as the origin of the atomic displacements, the D_{3d}-symmetric equilibrium configuration with the O_i at the center of symmetry (Fig. 1). Using Cartesian coordinate axes shown in Fig. 1, we express the displacement of the O_i by $(x,y,z) \equiv (r\cos\phi, r\sin\phi, z)$, and that of the jth silicon atom by $\boldsymbol{q}_j$. In accordance with Bosomworth *et al.*,[5] we take, as an unperturbed (uncoupled) system, the free excitation due to the (x,y) freedom of motion of the O_i in the static host lattice:

$$H^0=-\frac{\hbar^2}{2m}\left[\frac{1}{r}\frac{\partial}{\partial r}\left[r\frac{\partial}{\partial r}\right]+\frac{1}{r^2}\frac{\partial^2}{\partial\phi^2}\right]+v(r)\ , \tag{1}$$

$$v(r)=\alpha r^2+\beta r^4\ , \tag{2}$$

where m is the mass of the oxygen atom, and $v(r)$ is the static host lattice potential with the ϕ dependence neglected. Bosomworth *et al.*[5] employed, as $v(r)$, the Gaussian-bump-perturbed parabolic potential with three parameters. *Ab initio* electronic calculations[15,16] suggest that the ϕ-dependent potential terms are negligible.

We approximate the excitation due to $(z,q_1,q_2,\ldots)$ by a system of harmonic vibrations, and assume that an A_{2u} mode [Fig. 2(a)] of these vibrations is localized. This assumption accords with the experimental fact: existence of the high-energy bands due to the A_{2u} (z-like) transition dipole (Table I). We express the Hamiltonian of this A_{2u} local vibration as

$$H^{A_{2u}}=\hbar\omega_{A_{2u}}(b^\dagger_{A_{2u}}b_{A_{2u}}+\tfrac{1}{2})\ . \tag{3}$$

We take into account only the relevant part of the interaction terms between (x,y) and $(z,q_1,q_2,\ldots)$:

$$W^{A_{2u}}=g_{A_{2u}}r^2Q^2_{A_{2u}}\ , \tag{4}$$

where $g_{A_{2u}}$ is the coupling constant, and Q_{A2u} is the normal coordinate of the A_{2u} local mode, $Q_{A_{2u}}=\sqrt{(\hbar/2\omega_{A_{2u}})}(b^\dagger_{A_{2u}}+b_{A_{2u}})$.

We deal with the total Hamiltonian

$$\mathcal{H}\equiv H^0+H^{A_{2u}}+W^{A_{2u}}\ . \tag{5}$$

The $\mathcal{H}$ contains four unknown adjustable parameters α, β, $\hbar\omega_{A_{2u}}$, and $g_{A_{2u}}$. The values of α and β should be the same for all isotopic oxygens. The $\omega_{A_{2u}}$ depends on the mass m of the O_i, since $Q_{A_{2u}}$ generally contains the z displacement of the O_i. The $g_{A_{2u}}$ also depends on m, because $Q_{A_{2u}}$ is defined by a form containing m and M (mass of the silicon atom): $Q_{A_{2u}}=c_0\sqrt{m}z+\sum_{j,\kappa}c_{j\kappa}\sqrt{M}q_{j\kappa}$ $(\kappa=x,y,z)$, where $c_0^2+\sum_{j,\kappa}c_{j\kappa}^2=1$. If the A_{2u} mode completely localizes at the O_i, $\mathcal{H}$ describes a three-dimensional one-body motion of the O_i in the potential $v(r)+(m\omega^2_{A_{2u}}/2)z^2+mg_{A_{2u}}r^2z^2$. The electric dipole interaction with the applied electric field (E_x,E_y,E_z) is written as $e^*r(E_x\cos\phi+E_y\sin\phi)+M^*_{A_{2u}}E_zQ_{A_{2u}}$, where e^* and $M^*_{A_{2u}}$ are the constants. We use this to deal with the optical transitions.

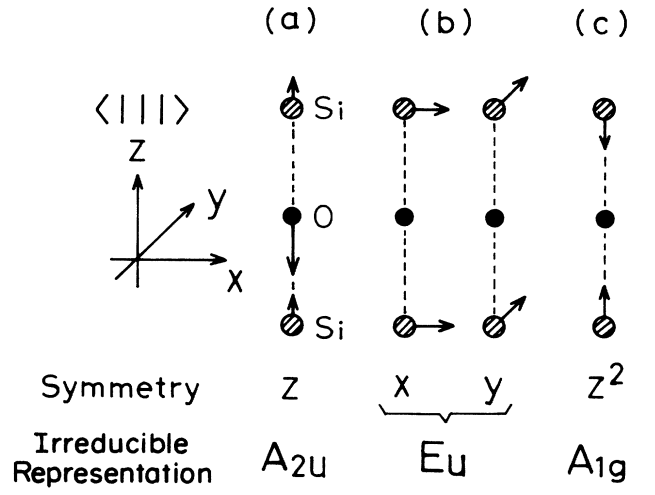

FIG. 2. Displacements of the O_i and the nearest silicon atoms in the normal modes belonging to the A_{2u}, E_u, and A_{1g} irreducible representations of the D_{3d} point group. Note that the normal modes have been defined in the excitation system that does not involve the (x,y) freedom of motion of the O_i (Sec. II).

Now we show the method of calculation. Neglecting the higher-order perturbation part

$$w'\equiv\tfrac{1}{2}(\hbar g_{A_{2u}}/\omega_{A_{2u}})r^2[(b^\dagger_{A_{2u}})^2+b^2_{A_{2u}}] \tag{6}$$

in $W^{A_{2u}}$, we approximate it by the remaining part:

$$w^{A_{2u}}\equiv(\hbar g_{A_{2u}}/\omega_{A_{2u}})r^2(b^\dagger_{A_{2u}}b_{A_{2u}}+\tfrac{1}{2})\ . \tag{7}$$

We can show that the level separation change due to w' is two orders of magnitude smaller than that due to $w^{A_{2u}}$, in the case of the present problem. Because the A_{2u} phonon number N, as well as the z-axial angular momentum l $(=0,\pm1,\pm2,\ldots)$, is the good quantum number of $H^0+H^{A_{2u}}+w^{A_{2u}}$, its eigenenergy $E_{kl,N}$, and eigenfunction

$$\Psi_{kl,N}=\phi_{kl,N}(r,\phi)|N\rangle$$
$$=\xi_{k|l|,N}(r)e^{il\phi}|N\rangle(b^\dagger_{A_{2u}}b_{A_{2u}}|N\rangle=N|N\rangle)$$

are obtained from the following equation in each subspace of N:

$$\mathcal{H}_N\phi_{kl,N}(r,\phi)=[E_{kl,N}-(N+\tfrac{1}{2})\hbar\omega_{A_{2u}}]\phi_{kl,N}(r,\phi)\ . \tag{8}$$

Here, $\mathcal{H}_N$ is the Hamiltonian with the renormalized potential

$$v_N(r)\equiv[\alpha+(\hbar g_{A_{2u}}/\omega_{A_{2u}})(N+\tfrac{1}{2})]r^2+\beta r^4 \tag{9}$$

substituted for $v(r)$ in (1). The label $k(=0,1,2,\ldots)$ distinguishes eigenstates $|k,l,N\rangle$ with the same (l,N). Here we see that the interaction $w^{A_{2u}}$ is renormalized into the coefficient α of $v(r)$. The renormalized part $v_N(r)-v(r)=(\hbar g_{A_{2u}}/\omega_{A_{2u}})(N+1/2)r^2$ can be shown to be an adiabatic potential[17] contributed from $w^{A_{2u}}$.

We solve Eq. (8) by numerically diagonalizing the matrix of $\mathcal{H}_N$ represented by the normalized eigenfunctions of a 2D harmonic oscillator, $\xi_{k|l|}(r)e^{il\phi}$. Thus, we obtain the radial part as

$$\xi_{k|l|,N}(r)\approx\sum_{k'}C^{(|l|,N)}_{k'k}\xi_{k'|l|}(r)\ . \tag{10}$$

We used 20–60 basis functions for each (l,N), and then ascertained that the calculated energy eigenvalues converged to 7–5 significant figures. Bosomworth *et al.*[5] employed the perturbation method for the center bump of the potential to solve the equation for the 2D LEAE.

III. PARAMETER DEPENDENCE OF THE ENERGY-LEVEL SCHEME

Regarding α, β (>0), and the impurity mass m as parameters, we investigate the dependence of the energy-level scheme of H^0 on these parameters. By using the dimensionless distance $R \equiv r(2m\beta/\hbar^2)^{1/6}$, H^0 in (1) is rewritten as follows:

$$H^0 = E_{\text{uni}} \left\{ -\left[\frac{1}{R}\frac{\partial}{\partial R}\left[R\frac{\partial}{\partial R}\right] + \frac{1}{R^2}\frac{\partial^2}{\partial\phi^2}\right] + A_{\text{non}}R^2 + R^4 \right\}, \tag{11}$$

where $E_{\text{uni}} \equiv [\hbar^4\beta/(2m)^2]^{1/3}$ is the scale of energy, and $A_{\text{non}} \equiv \alpha[2m/(\hbar\beta)^2]^{1/3}$ is a parameter that characterizes the picture of the excitation. We express the eigenenergy of H^0 as E_{kl}, and the coordinate of the minimum point of $v(r)$ as r_{min}. The solid curves in Fig. 3 show the A_{non} dependence of the normalized eigenenergy relative to the potential minimum, $[E_{kl} - v(r_{\text{min}})]/E_{\text{uni}}$, calculated by the method shown in Sec. II. The dotted curve indicates the normalized excitation energy $\hbar\omega_{\text{min}}/E_{\text{uni}}$ of the radial harmonic oscillation at r_{min}, where $\omega_{\text{min}} \equiv \{[d^2v(r)/dr^2]_{r=r_{\text{min}}}/m\}^{1/2}$. The dashed curve indicates the normalized height of the center bump relative to the potential minimum, $-v(r_{\text{min}})/E_{\text{uni}}$. The limits of $A_{\text{non}} \to +\infty$ and $-\infty$ correspond, respectively, to the harmonic oscillation and the rigid rotation. The region $0 \le A_{\text{non}}$ corresponds to the on-center anharmonic excitation, and the region $A_{\text{non}} < 0$ to the off-center excitation. In the region of strong off-center nature, $A_{\text{non}} \lesssim -10$, the picture of the excitation is the potential-ditch-confined vibrating rotation.

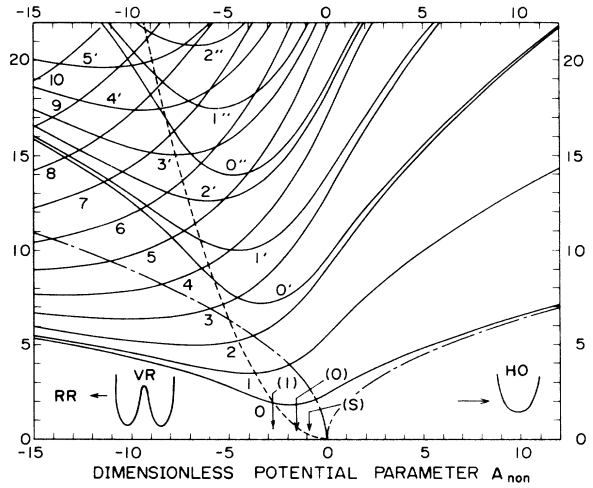

FIG. 3. The normalizeed eigenenergy $[E_{kl} - v(r_{\text{min}})]/E_{\text{uni}}$ as a function of the potential parameter A_{non}(solid curves). The figure also shows normalized excitation energy of the radial harmonic oscillation defined at r_{min}(dotted curve), and the normalized center bump height relative to the potential minimum (dashed curve). Symbols, 0, 1, . . . , 0′, 1′, . . . , 0″, 1″, . . . by each solid curve show the values of (k,l), e.g., the symbols 0, 0′, and 1′ mean $(k,l)=(0,0)$, $(1,0)$, and $(1,\pm1)$, respectively. The arrows on the abscissa with symbols (s), (0), and (1) indicate, respectively, the values of A_{non} in the problem of ^{16}O in $v(r)$, $v_0(r)$, and $v_1(r)$ shown in Fig. 5. The symbols HO, RR, and VR express the picture of the motion: the harmonic oscillation (HO), rigid rotation (RR), and vibrating rotation (VR).

IV. RESULTS OF CALCULATION

Obtained parameter values are shown in Table II. The corresponding energy levels of $H^0 + H^{A_{2u}} + w^{A_{2u}}$, together with those of $H^0 + H^{A_{2u}}$, are described in Figs. 4(a) (^{16}O) and 4(b) (^{18}O). The peaks in the 30-, 1100-, and 1200-cm^{-1} bands (Table I) are assigned, respectively, to the transitions represented by the solid arrows in Fig. 4. The transition $|1,0,0\rangle \to |1,0,1\rangle$ may contribute a superimposed peak to the 1127.8-cm^{-1} (^{16}O) and the 1076.7-cm^{-1} (^{18}O) peaks. These calculated transitions well explain the experimental data in Table I. Disagreement between the calculated transition energy (Fig. 4) and the observed peak energy (Table I) is less than (1 cm^{-1})hc for nearly all peaks. Our level scheme and peak assignment are the same as those of Bosomworth *et al.* (Fig. 9 of Ref. 5). This confirms their arguments about the essential aspects of the excitation: the 2D LEAE in the ϕ-independent potential, and its coupling to the 1100-cm^{-1} local vibration.[5] Figure 5 shows the static host-lattice potential $v(r)$, and the renormalized potentials $v_0(r)$, $v_1(r)$ of ^{16}O and ^{18}O, with the origin of energy at each potential minimum. Although the center bump of $v(r)$ is lower than that calculated by Bosomworth *et al.*[5] (3.3 meV), the distance r_{min} of the potential minimum is close to theirs (0.22 Å). Eigenenergies other than those shown in Fig. 4 can be known from Fig. 3. For ^{16}O, we find $E_{\text{uni}} = 1.5849$ meV, and $A_{\text{non}} = -0.9009$, -1.5262, and -2.7769 for $v(r)$, $v_0(r)$, and $v_1(r)$, respectively. These values of A_{non} are indicated in Fig. 3.

The energies of the 1100-cm^{-1} band transitions shown in Fig. 4 were the same, without the coupling. The coupling with negative $g_{A_{2u}}$ (Table I) makes the shape of $v_1(r)$ wider than that of $v_0(r)$, as is seen from the values of r_{min} in Fig. 5. Hence, as shown in Fig. 4, the level separations between the one-A_{2u}-phonon states become smaller compared to the zero-phonon states. (This is the level-separation reduction in the one-phonon state which Bosomworth *et al.*[5] derived experimentally.) Thus the

TABLE II. Values of the parameters obtained for ^{16}O and ^{18}O in the ^{28}Si—O—^{28}Si defect structure. Instead of the values of $g_{A_{2u}}$, those for $\hbar g_{A_{2u}}/\omega_{A_{2u}}$ are shown for convenience. Note that we use 1 meV $= (8.065\,48$ cm$^{-1})hc$ for conversion, where h and c are Planck's constant and light velocity in vacuum.

Fitting parameters	^{16}O	^{18}O
α (meV/Å^2)	-17.4615	
β (meV/Å^4)	237.017	
$\hbar\omega_{A_{2u}}$ (meV)	142.767	135.899
$\hbar g_{A_{2u}}/\omega_{A_{2u}}$ (meV/Å^2)	-24.2392	-19.8842

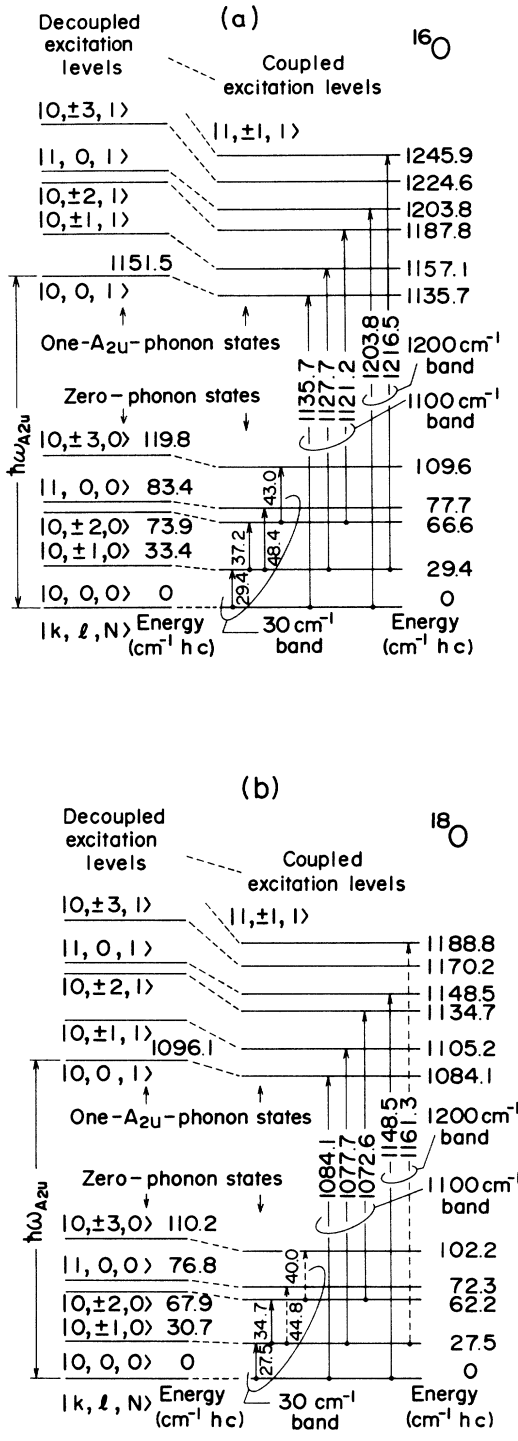

FIG. 4. Energy levels of $H^0+H^{A_{2u}}+w^{A_{2u}}$ (coupled excitation levels) and those of $H^0+H^{A_{2u}}$ (decoupled excitation levels) calculated for ^{16}O (a) and ^{18}O (b). The ground-state energy levels are drawn in the same energy position. The calculated eigenenergies relative to the ground state are shown at each level. The solid arrows indicate the transitions to which the peaks in the 30-, 1100-, and 1200-cm^{-1} bands (Table I) are assigned. Calculated transition energy is given in each arrow. The dashed arrows in (b) indicate the transitions which may be observed as peaks in case of higher ^{18}O concentration.

transition energy of the 1100-cm^{-1} band is smaller for the transition from the higher zero-phonon level (Fig. 4). This is how the multipeak structure of the 1100-cm^{-1} band appears. As has been pointed out by Bosomworth *et al.*,[5] the 1200-cm^{-1} band is regarded as a 2D LEAE sideband of the local-phonon transition, because k as well as N increases in the transition (Fig. 4). Also this sideband originates from the N dependence of $v_N(r)$ due to the coupling. The N dependence causes nonorthogonality $\langle \xi_{1|l|,1}|\xi_{0|l|,0}\rangle \neq 0$, which gives a nonzero probability to the sideband transition $|0,l,0\rangle \rightarrow |1,l,1\rangle$, as shown below. For low temperatures, the intensity of the 1100- and 1200-cm^{-1} absorptions is expressed as

$$I(k,l,0\rightarrow k',l,1)=(M^*_{A_{2u}})^2(\hbar/2\omega_{A_{2u}})\rho_{kl,0}(E_{k'l,1}-E_{kl,0}) \times |\langle \xi_{k'|l|,1}|\xi_{k|l|,0}\rangle|^2 , \quad (12)$$

with irrelevant factors omitted. Here, $\rho_{kl,0}$ is Boltzmann's occupation probability for the initial state $|k,l,0\rangle$. The radial integral in (12) defined by $\int_0^\infty dr\, r\xi_{k'|l|,1}(r)\xi_{k|l|,0}(r)$ corresponds to the phonon overlap integral in the problem of the localized electron-phonon system. For ^{16}O, the values of this integral calculated from (10) are 0.997, −0.999, −0.997, 0.062, and −0.008 for $(k',k,|l|)=(0,0,0)$, (0,0,1), (0,0,2), (1,0,0), and (1,0,1), respectively. Thus, $|\langle \xi_{10,1}|\xi_{00,0}\rangle / \langle \xi_{00,1}|\xi_{00,0}\rangle| = 0.062$. This value is about 30% smaller than that derived by applying (12) to the measured ratio of the peak absorbance between the 1203- and the 1136-cm^{-1} peaks.[9] These values, however, well explain that the measured intensities of the 1200-cm^{-1} band peaks are 2–3 orders of magnitude smaller than those of the 1100-cm^{-1} band.

As shown in Fig. 4, the level separation change due to the coupling is considerably large even in the zero-phonon states. To investigate the effect of the coupling on the isotope peak shift, we calculated the energy levels of ^{18}O in the renormalized potential $v_0(r)$ of ^{16}O shown in Fig. 5(b). This calculation corresponds to such a situation where the renormalization effect [the second term in the brackets of (9)] for ^{18}O is assumed to be the same as that for ^{16}O. We can also regard this calculation as a free 2D LEAE model with the potential assumed to be $v_0(r)$ of ^{16}O. This calculation estimated the ^{18}O isotope shifts of the 29.3- and 37.8-cm^{-1} peaks to be 2.7 and 3.1 cm^{-1}, respectively. Both of these are larger than the observed values: 2.1 and 2.5 cm^{-1} (Table I). Similar overestimation was given by the free 2D LEAE model of Bosomworth *et al.* (2.7 and 3.1 cm^{-1}).[5] Our model has resolved this overestimation, giving the values of 1.9 and 2.5 cm^{-1} (Fig. 4), which are much closer to the observed ones. This improvement has been brought about by taking into account the coupling which gives larger renormalization effect (i.e., larger potential-widening effect) to ^{16}O than to ^{18}O.

V. DISCUSSION

As seen from (9), the sign of the coupling constant $g_{A_{2u}}$ significantly affects the energy-level scheme. Here, we ex-

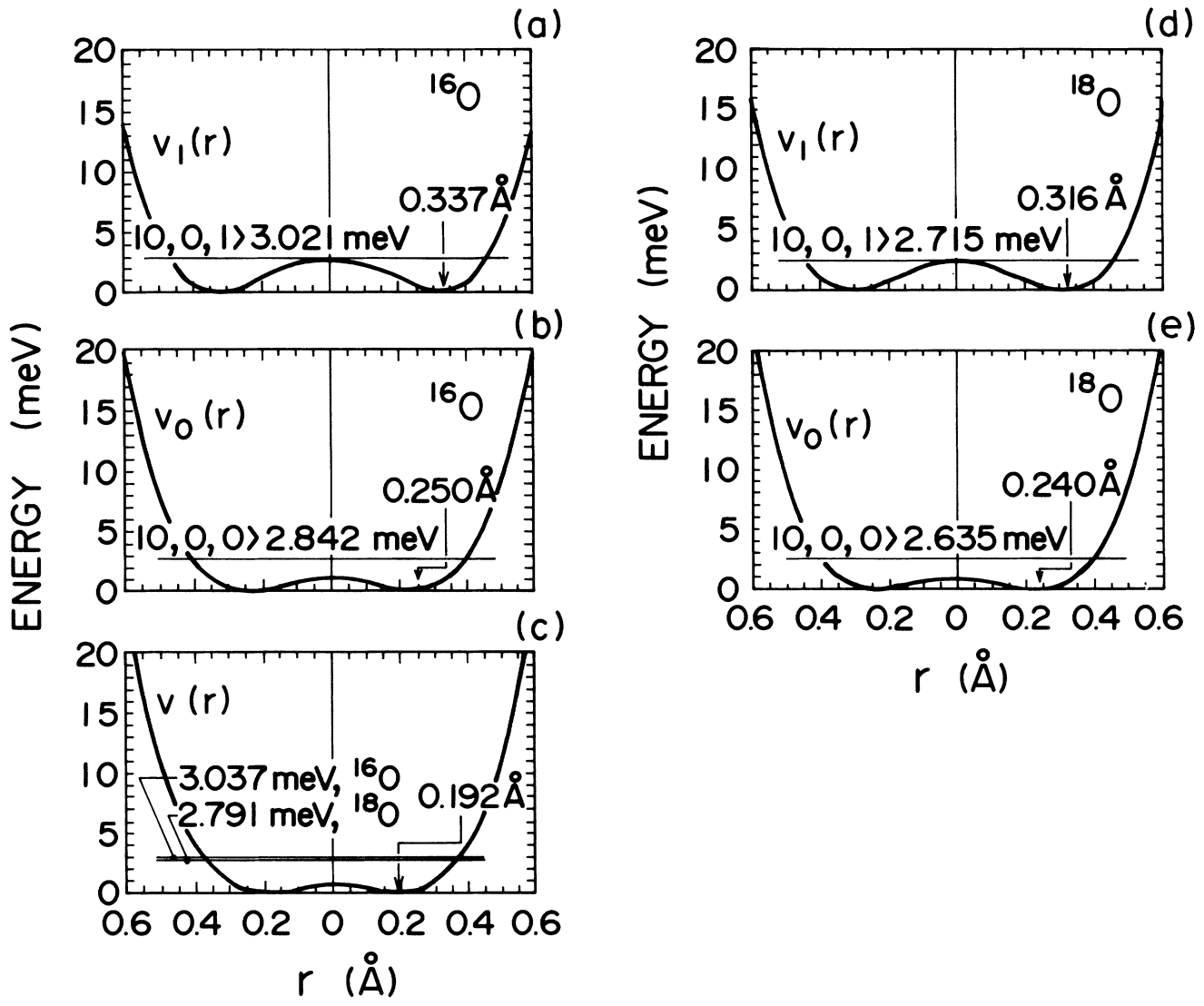

FIG. 5. Calculated static host-lattice potential (c), renormalized potentials of ^{16}O and ^{18}O in the zero-phonon state (b), (e), and those in the one-A_{2u}-phonon state (a), (d). The radial coordinate $r_{\min}$ of each potential minimum is indicated. Only the lowest energy level in each potential is described.

plain the physical origin of our result of negative $g_{A_{2u}}$. The total potential energy of our A_{2u}-mode-coupled 2D LEAE is the sum of the potential parts of H^0 and $H^{A_{2u}}$, and $W^{A_{2u}}$, that is, $E(Q_{A_{2u}},r)\equiv v(r)+(\omega^2_{A_{2u}}/2)Q^2_{A_{2u}}+g_{A_{2u}}r^2Q^2_{A_{2u}}$. Therefore, the "force constant" for the A_{2u}-mode displacement is expressed as $(\partial/\partial Q_{A_{2u}})^2E(Q_{A_{2u}},r)=\omega^2_{A_{2u}}+2g_{A_{2u}}r^2$. Thus, the negativeness of $g_{A_{2u}}$ indicates that the force constant becomes smaller for larger r. The actual Si—O—Si bond has this characteristic: the force constant for the bendinglike A_{2u}-mode displacement (Fig. 6) would be smaller than that for the pure stretching one [Fig. 2(a)], $\omega^2_{A_{2u}}$.[18] The present negative $g_{A_{2u}}$ is reflecting this physical property which issues from electronic mechanism.

Table I indicates that the 517-cm^{-1} absorption should be described by irreducible transition dipole operators (displacement operators) of (x,y)-like symmetry, which belong to the E_u representation of the D_{3d}. Consequently, if the interaction with the 2D LEAE is neglected, this absorption is attributed to an E_u mode [Fig. 2(b)] in the perturbed phonon system. The lowest-order interaction is of the form

$$W^{E_u}=g_{E_u}r[(\cos\phi)Q_{E_{u,x}}+\sin\phi Q_{E_{u,y}}]\,, \tag{13}$$

where $\{Q_{E_{u,x}},Q_{E_{u,y}}\}$ are the E_u normal coordinates. However, the 517-cm^{-1} absorption exhibits neither a multipeak structure nor a measurable ^{18}O isotope shift.[2] Thus, the coupling constant g_{E_u} is estimated as nearly zero. Consequently, this absorption is ascribed to the O_i-induced host-lattice mode belonging to the E_u.

The 1700-cm^{-1} band resembles the 1100-cm^{-1} band in the shape of the multipeak structure and its temperature dependence.[6,8,9] This implies that the 1700-cm^{-1} band is

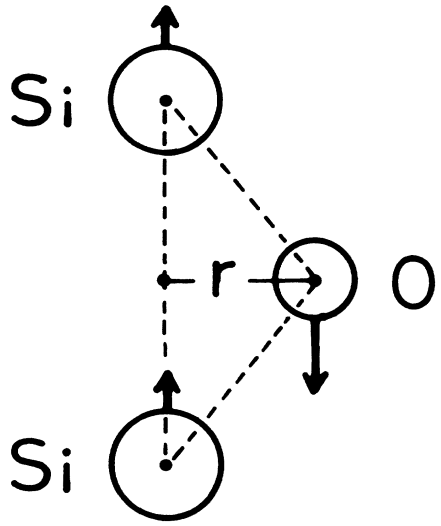

FIG. 6. The A_{2u} mode displacement for $r \neq 0$. The figure shows such atomic displacement that each atom displaces from an $r \neq 0$ configuration in accordance with the A_{2u} normal displacement $Q_{A_{2u}}$ defined at $r=0$ [Fig. 2(a)].

a replica of the 1100-cm^{-1} band which originates from the A_{2u}-mode-coupled 2D LEAE ($\mathcal{H}$) further coupled to another excitation of an energy of about 613 cm^{-1}hc. The silicon isotope shifts of the 1748.6-cm^{-1} peak due to ^{x}Si—O—^{28}Si (-6.4, -13.2 cm^{-1} for $x=29$, 30)[9] are considerably larger than those of the 1136-cm^{-1} peak. (-1.8, -3.5 cm^{-1}).[4,5] This implies that "another excitation" is a localized mode having large amplitude at the nearest Si, rather than the bulk phonons speculated previously.[8] A candidate for it is an A_{1g} mode [Fig. 2(c)], which, combined with $\mathcal{H}$ by the coupling $g_{A_{1g},A_{2u}} Q_{A_{1g}} Q^2_{A_{2u}}$, reproduces the 1700-cm^{-1} band as the one-A_{1g}-phonon replica of the 1100-cm^{-1} band. This explanation is, however, a speculation, and not the result of the present theoretical treatment.

VI. SUMMARY AND CONCLUSIONS

To consistently explain the previously observed 30-, 1100-, and 1200-cm^{-1} absorption bands, the coupling to the A_{2u} local phonon has been added to the 2D one-body excitation model of Bosomworth *et al.*,[5] which treated only the 30-cm^{-1} band. We obtained, for both ^{16}O and ^{18}O, the energy levels (Fig. 4) that explain the experimental data for these bands (Table I). Our level scheme and transition assignment are the same as those of Bosomworth, *et al.* (Fig. 9 of Ref. 5). We clarified how the coupling causes the 1200-cm^{-1} band and the multipeak structure of the 1100-cm^{-1} band. The calculated relative intensity of the 1200-cm^{-1} band was in satisfactory agreement with experiment. The coupling considerably reduces the level separations of the 2D excitation, depending on the oxygen mass. This is an important factor in explaining the ^{18}O isotope shifts of the peaks. The negative sign of the calculated coupling constant reflects the physical property of the Si—O—Si bond. The 517-cm^{-1} absorption was ascribed to the O_t-induced host-lattice mode of the E_u symmetry.

ACKNOWLEDGMENTS

One of the authors (H. Y. -K.) would like to thank Dr. Y. Kayanuma of Tohoku University for valuable discussions. The authors are also grateful to H. Tsuchikawa and K. Wada of Fujitsu Limited for their encouragement.

[1]H. J. Hrostowski and R. H. Kaiser, Phys. Rev. **107**, 966 (1957).
[2]H. J. Hrostowski and B. J. Alder, J. Chem. Phys. **33**, 980 (1960).
[3]J. W. Corbett, R. S. McDonald, and G. D. Watkins, J. Phys. Chem. Solids **25**, 873 (1964).
[4]B. Pajot, J. Phys. Chem. Solids **28**, 73 (1967).
[5]D. R. Bosomworth, W. Hayes, A. R. L. Spray, and G. D. Watkins, Proc. R. Soc. London Ser. A **317**, 133 (1970).
[6]A. K. Krishnan and S. L. Hill, in *Proceedings of the 1981 International Conference on Fourier Transform Infrared Spectroscopy, Columbia, 1981,* edited by H. Sakai (The International Society for Optical Engineering, Bellingham, WA, 1981), p. 27.
[7]M. Stavola, Appl. Phys. Lett. **44**, 514 (1984).
[8]B. Pajot, H. J. Stein, B. Cales, and C. Naud, J. Electrochem. Soc. **132**, 3034 (1985).
[9]B. Pajot and B. Cales, in *Materials Research Society Symposia Proceedings, Boston, 1985,* edited by J. C. Mikkelsen, Jr., S. J. Pearton, J. W. Corbett, and S. J. Pennycook (Materials Research Society, Pittsburgh, 1986), Vol. 59, p. 39.
[10]A. S. Oates and M. Stavola, J. Appl. Phys. **61**, 3114 (1987).
[11]A. M. Stoneham, in *Theory of Defects in Solids* (Clarendon, Oxford, 1975), pp. 224 and 710.
[12]W. Hayes and A. M. Stoneham, in *Defects and Defect Processes in Nonmetallic Solids* (Wiley, New York, 1985), p. 83.
[13]M. Stavola, S. J. Pearton, J. Lopata, and W. C. Dautremont-Smith, Phys. Rev. B **37**, 8313 (1988).
[14]H. Yamada-Kaneta, C. Kaneta, T. Ogawa, and K. Wada, Mater. Sci. Forum **38-41**, 637 (1988).
[15]C. Kaneta, H. Yamada-Kaneta, and A. Osawa, Mater. Sci. Forum **38-41**, 323 (1988).
[16]E. Martinez, J. Plans, and F. Yndurain, Phys. Rev. B **36**, 8043 (1987).
[17]A. M. Stoneham, in Ref. 11, p. 373.
[18]This is shown by an *ab initio* electronic calculation with the same model as in Ref. 15. The details are planned to be presented elsewhere by C. Kaneta *et al.*